



Effective Measuring Area and Test Protocol in Picture Frame Method to Measure In-plane Shear Modulus of Cross-laminated Timber

Jiyong KIM¹ · Kyung-Sun AHN¹ · Sung-Jun PANG² · Da-bin SONG³ · Chul-Ki KIM³ · Kwangmo KIM⁴ · Kugbo SHIM⁵ · Keon-Ho KIM^{6,†} · Jung-Kwon OH^{7,†}

ABSTRACT

This study established a standardized test method for the in-plane shear modulus of cross-laminated timber (CLT) KS F 2082. Among the test methods used to evaluate the in-plane shear modulus of CLT, the picture frame method was considered appropriate for achieving a pure shear state. However, the test procedures for the picture frame method have varied among studies owing to the lack of a standardized test method. Therefore, the deformation measurement area and loading protocol are discussed herein. The measurement area was determined based on the shear behavior of the test specimens using digital image correlation. The tensile and compressive deformations were similar when the side measurement area length was less than 70% of the side length of the test specimen. In addition, a three-stage loading protocol, including a two-step preloading, was proposed to settle the specimen during loading. Testing of a plywood panel showed that the difference between tensile and compressive deformations decreased as the stages progressed. Considering the larger difference in the first phase compared to the subsequent phases, it was concluded that at least one preloading step was required to achieve a pure shear state. A CLT specimen was tested following these procedures and exhibited linear load-deformation curves with a small difference (2.0%) in the tensile and compressive directions. Therefore, the test procedure proposed in KS F 2082 appears to be suitable for achieving a pure shear state and is an effective testing method for CLT.

Keywords: cross-laminated timber, in-plane shear modulus, massive wood panel, picture frame method, effective loading protocol

Date Received August 23, 2024; Date Revised September 9, 2024; Date Accepted October 29, 2024; Published November 25, 2024

¹ Department of Agriculture, Forestry and Bioresources, Seoul National University, Seoul 08826, Korea

² Department of Wood Science and Engineering, Chonnam National University, Gwangju 61186, Korea

³ Wood Engineering Division, National Institute of Forest Science, Seoul 02455, Korea

⁴ Research Planning and Coordination Division, National Institute of Forest Science, Seoul 02455, Korea

⁵ Department of Wood and Paper Science, Chungbuk National University, Cheongju 28644, Korea

⁶ Wood Industry Division, National Institute of Forest Science, Seoul 02455, Korea

⁷ Department of Agriculture, Forestry and Bioresources/Research Institute of Agriculture and Life Sciences, Seoul National University, Seoul 08826, Korea

† Corresponding author: Keon-Ho KIM (e-mail: keon@korea.kr, <https://orcid.org/0000-0001-6423-164X>)

† Corresponding author: Jung-Kwon OH (e-mail: jungoh@snu.ac.kr, <https://orcid.org/0000-0002-8776-0955>)

© Copyright 2024 The Korean Society of Wood Science & Technology. This is an Open-Access article distributed under the terms of the Creative Commons Attribution Non-Commercial License (<http://creativecommons.org/licenses/by-nc/4.0/>) which permits unrestricted non-commercial use, distribution, and reproduction in any medium, provided the original work is properly cited.

1. INTRODUCTION

Owing to climate change and global warming, interest in timber structures has increased because of their sustainability and decreased carbon emissions compared to other building materials (Cha *et al.*, 2022; Hwang *et al.*, 2022; Kang *et al.*, 2023; Lee and Oh, 2023; Oh, 2022; Oh *et al.*, 2023; Ozdemir *et al.*, 2023). In particular, cross-laminated timber (CLT), an engineered wood panel, is widely used in mid- and high-rise timber buildings because of its mechanical properties and applicability in prefabrication (Ha *et al.*, 2023; Kim *et al.*, 2024; Song and Kim, 2022, 2023; Trisatya *et al.*, 2023).

One issue with mid- and high-rise buildings is their resistance to lateral forces caused by wind or earthquakes (Lee and Jang, 2023). Structural analysis simulations that require in-plane shear properties as input data are necessary for designing tall buildings to model the behaviors of shear walls and diaphragms. When CLT are used for shear walls or diaphragms, the in-plane shear modulus is an important property (Berg *et al.*, 2019; Lukacs *et al.*, 2019). Therefore, a method to measure the in-plane shear stiffness of CLT is required.

The in-plane shear behavior of CLT can be distinguished by three principal mechanisms: net shear, tor-

sional shear, and gross shear, as illustrated in Fig. 1 (Bogensperger *et al.*, 2007; Brandner *et al.*, 2013; Flaig and Blaß, 2013). Several studies have investigated these mechanisms through single-node tests using small specimens (Brandner *et al.*, 2013; Jöbstl *et al.*, 2008; Wallner, 2004). However, while the single-node test is suitable to analyze the failure modes of small specimens, this method is inappropriate to represent the in-plane shear behavior or evaluate the in-plane shear modulus of a full-scale CLT panel (Andreolli *et al.*, 2014; Björnfot *et al.*, 2017). Even if the in-plane shear modulus of CLT could be measured using small specimens, a verification method is necessary to ensure that this value is applicable to large CLT panels. Therefore, to properly evaluate the in-plane shear modulus of the CLT, large-scale test of CLT panels have been conducted.

Using large-scale CLT panels, various methods for evaluating the in-plane shear properties have been proposed, such as column compression, diagonal compression, double shear, and picture frame, as shown in Fig. 2 (Andreolli *et al.*, 2014; Berg *et al.*, 2019; Björnfot *et al.*, 2017; Bogensperger *et al.*, 2007; Bosl, 2002; Brandner *et al.*, 2013; Dujic *et al.*, 2007; Gubana, 2008; Kreuzinger and Sieder, 2013; Turesson *et al.*, 2019a, 2019b).

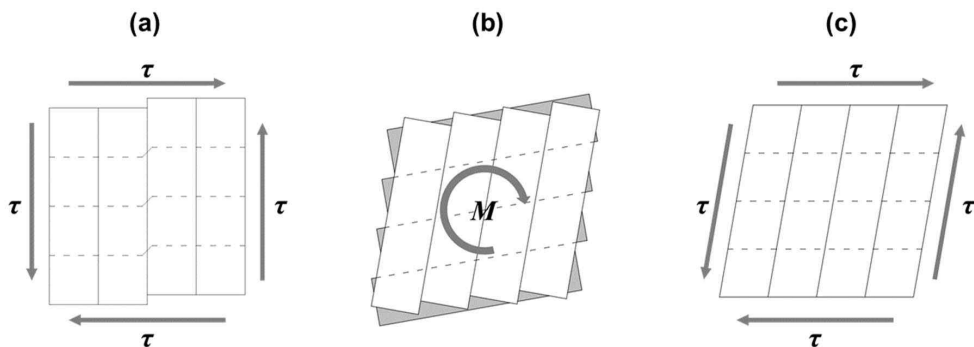


Fig. 1. Configuration of the in-plane behavior of CLT. (a) Net shear, (b) torsional shear, and (c) gross shear. CLT: cross-laminated timber.

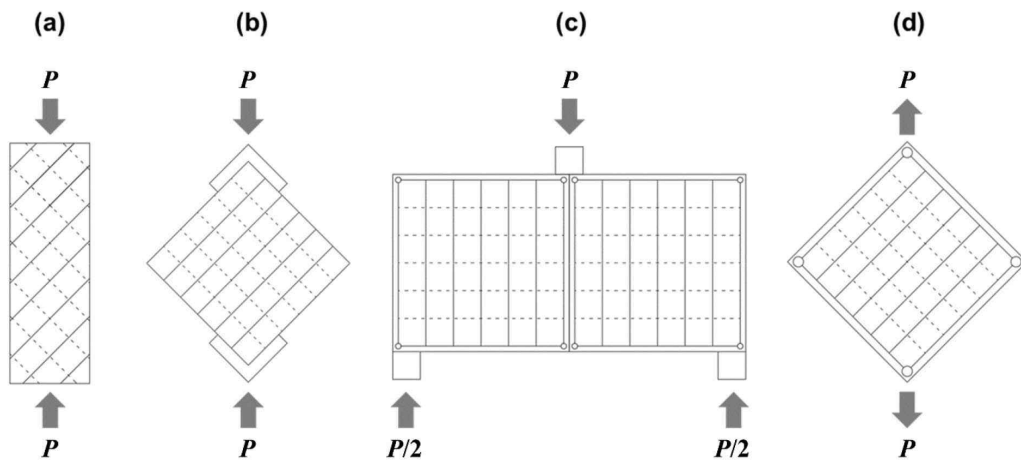


Fig. 2. Test configurations of larger-scale CLT panels. (a) Column compression, (b) diagonal compression, (c) double shear, and (d) picture frame method. CLT: cross-laminated timber.

Kreuzinger and Sieder (2013) proposed the column compression method to evaluate the in-plane shear modulus of the CLT panel [Fig. 2(a)], whereas Andreolli *et al.* (2014) and Dujic *et al.* (2007) proposed the diagonal compression method [Fig. 2(b)]. The column compression and diagonal compression methods use only compressive load to create the shear stress in the specimen. In these methods, the CLT specimen is installed at an angle of 45° , and the compressive stress acts as a shear stress. However, compressive stress exists in the specimen in addition to shear stress. Therefore, it has been argued that a pure-shear state was not achieved. Turesson *et al.* (2019b) reported that these methods might overestimate the in-plane modulus of the CLT owing to the nonuniform shear deformation of the panels. In the double shear method proposed by Bogensperger *et al.* (2007) [Fig. 2(c)], the stress state of the specimen could not be considered as a pure shear state because a moment occurred in the specimens owing to the load introduction. Since the in-plane shear modulus should ideally be evaluated in the pure shear state, a method that can introduce pure shear in the test specimen is required.

The picture frame method uses several steel frames that are connected to each other by a pin joint, and transfers the load to the specimen using friction, glue, dowels, and bolts (Björnfort *et al.*, 2017; Bogensperger *et al.*, 2007; Bosl, 2002). Turesson *et al.* (2019b) reported that the difference in deformation between the compressive and tensile directions in the picture frame method was smaller than that in the diagonal compression method because the picture frame can apply compressive and tensile stresses to the specimen simultaneously. This indicates that the stress induced by the picture frame method is closer to the pure shear state than those induced by the other methods. Turesson *et al.* (2019b) reported that the picture frame method is a testing method that can be used to achieve an approximation of a pure shear state.

However, the picture frame method involves a deformation measurement area. The deformation measurement area is the region where the deformation of the specimen is measured using a displacement transducer. Because stress concentration could occur near the connections between the picture frame and the test specimen, a pure shear state may not occur in the entire area of the test

specimen. Andreolli *et al.* (2014), Berg *et al.* (2019), Björfot *et al.* (2017), and Turesson *et al.* (2019b) set the deformation measurement area length to 0.4 times the specimen side length (Fig. 3), and Bogensperger *et al.* (2007) reported that a large measurement area could lead to an inaccurate estimation of the shear modulus. Thus, a discussion of the measurement area of the picture frame method is required.

Another issue with the picture frame method is the loading protocol used. Berg *et al.* (2019), Björfot *et al.* (2017), and Turesson *et al.* (2019b) applied preloading to minimize the effect of fastener tolerance, which reduced the difference between the tensile and compressive directions in subsequent loading phases. However, loading protocols varied across these studies. Therefore, in addition to the measurement area, the loading protocol must also be examined.

This study investigated test method for the in-plane shear modulus of CLT, particularly the measurement area and loading protocol. The measurement area and loading protocol were determined by tests on an acrylic sheet and plywood panel, which are relatively isotropic mate-

rials compared to CLT. The test methods were then verified using a CLT panel. Based on these results, KS F 2082 (Korean Standards Association, 2023), a test standard to evaluate the in-plane shear modulus of CLT, was issued in 2023. This study supported the KS committee by providing research evidence.

2. MATERIALS and METHODS

2.1. Raw materials

To determine the measurement area, a preliminary test was conducted using a 20 mm-thick acrylic sheet (ClearWhite; AltuglasTM, Paris, France). An acrylic sheet was considered because it is a more isotropic material than CLT. A 24 mm thick structural plywood panel was used to determine the optimal loading protocol. The grade of the plywood panel was class 1, according to KS F 3113 (Korean Standards Association, 2021), and was composed of nine layers of Japanese Larch (*Larix kaempferi carr.*; Sun & L, Incheon, Korea). The configurations of the acrylic sheet and plywood panel are shown in Fig. 4(a). The corners and holes were cut using a CNC machine with a 1 mm tolerance for mounting and demounting the bolts and dowels. The CLT panel was composed of Japanese Larch (*L. kaempferi carr.*) and glued using Phenol-Resorcinol Formaldehyde resin without edge gluing. It was 140 mm thick and had five layers. The configurations of the acrylic sheet and the plywood panel are shown in Fig. 4(b). The density of the CLT panel was 568 kg/m³ and the moisture content was 11.87%. The acrylic sheet, plywood panel and CLT panel were each tested once.

The picture frame was designed as described by Björfot *et al.* (2017) and Turesson *et al.* (2019b). The dimensions and configuration of the picture frame are shown in Figs. 5 and 6. It consisted of eight L-shaped steel beams with four beams per side. The thickness of the L-shaped beams was 14 mm. The L-shaped beams

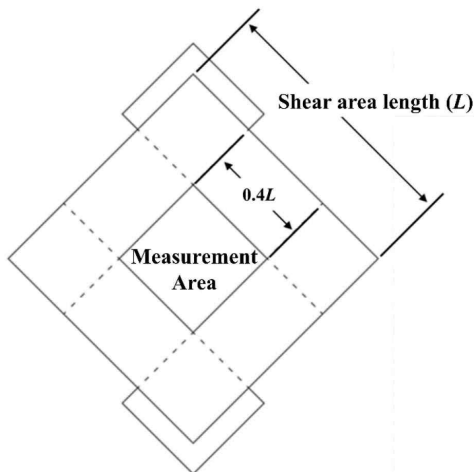


Fig. 3. Deformation measurement area proposed by Andreolli *et al.* (2014).

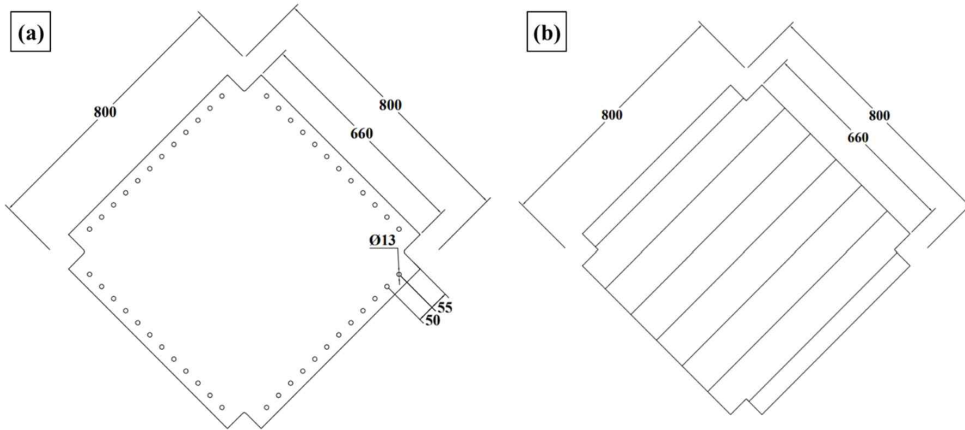


Fig. 4. Configuration of the test specimen. (a) Acrylic sheet/plywood panel and (b) CLT panel (unit: mm). CLT: cross-laminated timber.

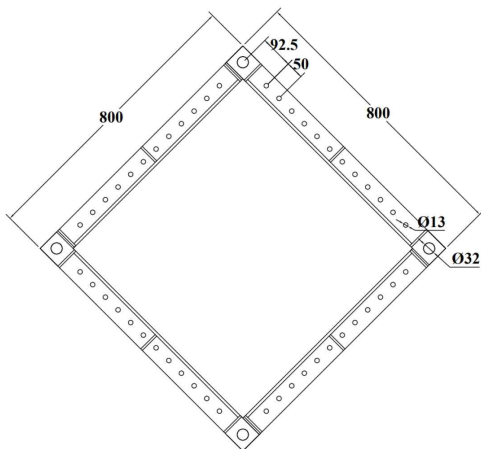


Fig. 5. Configuration of the picture frame (unit: mm).

were made of SS315 grade steel (Korean Standards Association, 2018), with a yield strength of 315 MPa. The holes for the panel fasteners were drilled with a 1 mm tolerance, and the holes for the frame connecting dowels were drilled with a 2 mm tolerance. To prevent splitting, the spacing between the holes was designed to be larger than four times the hole diameter, following KDS 41 50 30 (Ministry of Land, Infrastructure and Transport, 2022). The diameter of the dowel assembled

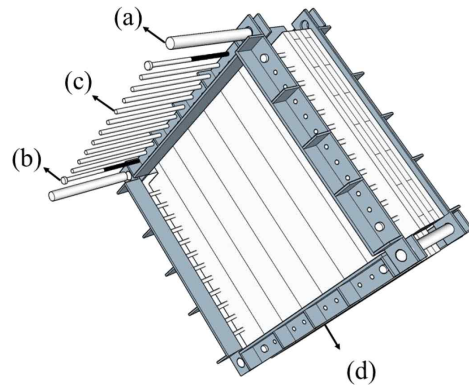


Fig. 6. Configuration of the test jig. (a) $\phi 30$ mm dowel to connect L-shaped beams, (b) $\phi 12$ mm bolt to prevent the picture frame from separating, (c) $\phi 12$ mm dowel, and (d) L-shaped beams.

between the L-shaped beams was 30 mm, and its tensile strength was 600 MPa. The specimens were mounted on the picture frame using dowels and bolts of 12 mm diameter. Eight bolts were used to prevent the picture frame from separating during the test (Fig. 6). When a tensile load was applied to the picture frame, this load was transferred to the test specimen by the picture frame and fasteners.

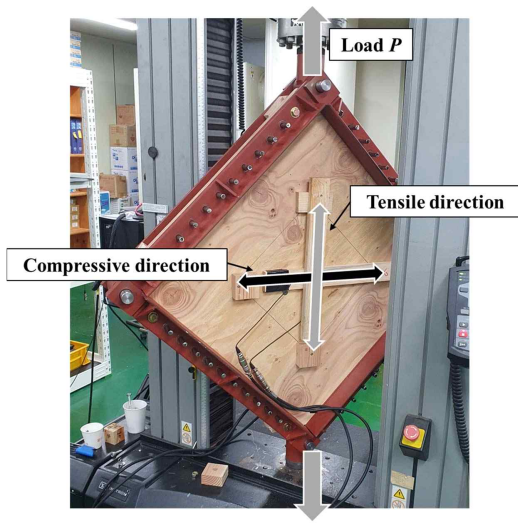


Fig. 8. Configuration of the plywood panel in-plane shear test.

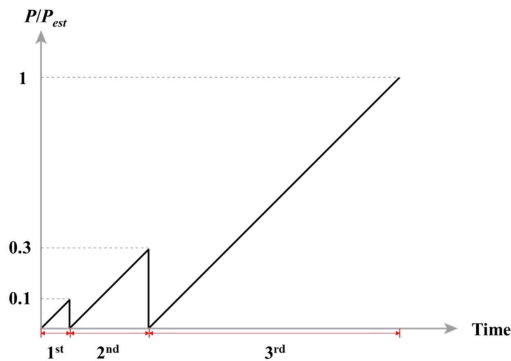


Fig. 9. Three-stage loading protocol. Where P_{est} : Estimated maximum load, which can be evaluated by a preliminary test or by the shear strength and area of the test specimen.

study. The achievement of a pure shear state in the CLT specimens was examined from the test results. A formula for the in-plane shear modulus of CLT was derived. In-plane shear modulus G is defined as shear stress (τ) divided by shear strain (γ). Shear stress was determined using the shear force and shear area [Equation (2)]. The applied load, shear force, specimen thickness, and shear

area length are shown in Fig. 10.

$$\tau = \frac{F}{A} = \frac{\frac{P}{\sqrt{2}}}{t \times L} = \frac{P}{tL\sqrt{2}} \quad (2)$$

Where τ : shear stress (N/mm²), F : shear force (N), A : shear area (mm²), P : applied load (N), t : thickness of specimen (mm), L : shear area length (mm; Fig. 10).

When a load (P) was applied to the panel, the measured area deformed, as shown in Fig. 11. Using the law of cosines, Fig. 11 can be described using Equation (3). The in-plane shear modulus can be calculated using Equations (3) to (6):

$$(L_m \sqrt{2} + \Delta)^2 = L_m^2 + L_m^2 - 2L_m^2 \cos(90 + \gamma) \quad (3)$$

$$\cos(90 + \gamma) = -\sin \gamma \approx -\gamma, \Delta^2 \approx 0 \quad (4)$$

$$\gamma = \frac{\Delta \sqrt{2}}{L_m} \quad (5)$$

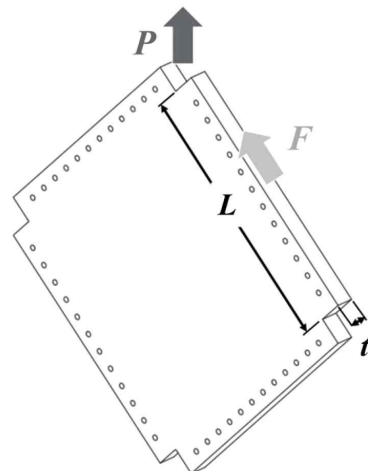


Fig. 10. Schematic drawing of the panel with applied load (P), shear force (F), thickness of the specimen (t), and shear area length (L).

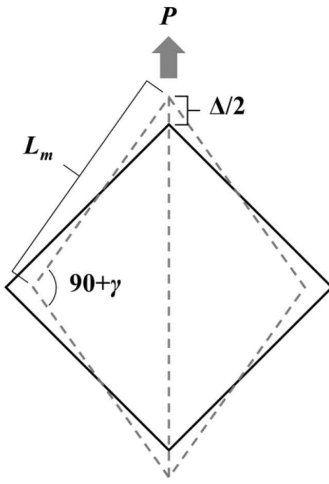


Fig. 11. Deformation of the measurement shear area.

$$G = \frac{\tau}{\gamma} = \frac{\frac{P}{tL\sqrt{2}}}{\frac{\Delta\sqrt{2}}{L_m}} = \frac{P}{\Delta} \frac{L_m}{L} \frac{1}{2t} \quad (6)$$

Where L_m : measurement area length (mm), Δ : deformation in diagonal (mm), γ : shear strain (rad), G : shear modulus (MPa).

Because the deformations were measured in the tensile and compressive directions, both directions must be considered when evaluating the in-plane shear modulus. Berg *et al.* (2019) and Turesson *et al.* (2019b) proposed a method that averages the slopes of the load-deformation curves in both directions instead of simply averaging the deformations to evaluate the in-plane shear modulus. Therefore P/Δ , which indicates the slope of the curve, was defined in Equation (7). In addition, Equation (6) is rewritten as Equation (8) by averaging the slopes in both directions. In KS F 2082, Equation (8) was proposed to evaluate the in-plane shear modulus of the CLT.

$$k_i = \frac{P}{\Delta_i} \quad (7)$$

$$G = \frac{k_c + k_t}{2} \frac{L_m}{L} \frac{1}{2t} \quad (8)$$

Where Δ_i : deformation in the i -direction (mm; i : compressive or tensile), k_i : slope of curve in the i -direction (N/mm; i : compressive or tensile), k_c : slope of the curve in the compressive direction (N/mm), k_t : slope of the curve in the tensile direction (N/mm).

3. RESULTS and DISCUSSION

3.1. Determination of measurement area

Fig. 12 shows that the difference between the tensile and compressive deformations decreases from the edge toward the center. Within 70% of the shear length (points 6–9 in Fig. 7), the difference between the tensile and compressive deformations is less than 10%. These results suggest that the in-plane shear modulus can be measured over a range greater than 40% of the shear length, as previously suggested (Andreolli *et al.*, 2014; Berg *et al.*, 2019; Björnöt *et al.*, 2017; Turesson *et al.*, 2019b). Conservatively, it is stipulated that the measurement area for determining the shear modulus should be set within a maximum of 50% of the shear length in the standardized test method in KS F 2082.

3.2. Determination of loading protocol

Fig. 13 shows the load-deformation curve of the acrylic sheet test. An unstable region was observed below the 50 kN load line, highlighting the need for preloading. The preloading phase stabilized the displacement transducer and connections between the picture frame and test specimen (Turesson *et al.*, 2019b).

The plywood panel was therefore tested following the loading protocol of three-stage load phases. The first load phase was from 0 to $0.1 P_{est}$, the second from 0 to $0.3 P_{est}$, and the third from 0 to P_{est} (Fig. 9). The first and second load phases were used to stabilize the initial

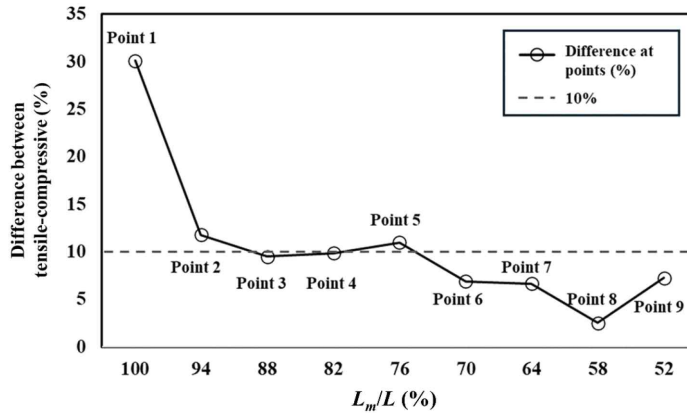


Fig. 12. Difference between tensile and compressive deformations at the measured points on acrylic sheet (L_m/L is the ratio between measurement area length at point m and shear area length, see Fig. 7).

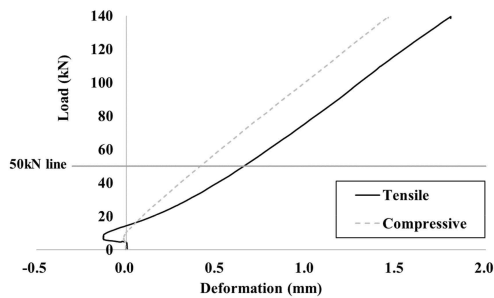


Fig. 13. Load-deformation curve of the acrylic sheet test.

disturbance. An estimated maximum load of 257.6 kN was determined based on the shear area and shear strength of the plywood panel, using the test data of Riberholt (1984).

Fig. 14 shows the load-deformation curves of the plywood panel. In Fig. 14(b) and (c), the linearity of the load-deformation curve can be seen compared with Fig. 14(a), the first load phase. Because the load-deformation curves of the second and third load phases showed similar behaviors, the two curves were compared in Fig. 15. Each curve shows the average load-deformation curves of the second and third load phases, representing the mean values of the tensile and compressive

curves. The load-deformation curve of the second load phase is seen to be very close to that of the third load phase.

Table 1 lists the slopes of the curves of the plywood specimens at each loading phase. The slopes of the load-deformation curves in all regions were evaluated using the least-squares method. In the first load phase, the slopes in the tensile and compressive directions were significantly different (36.1%), and a smaller difference was observed in the higher-step load phase (second load phase, 8.0%; third load phase, 7.3%). In the first load phase, there was a difference between the compressive and tensile slopes because of the gap between the jig and test specimen. In the second load phase, the effect of the gap was significantly reduced. Considering the large difference between the tensile and compressive directions, a loading protocol that introduces at least one preloading stage with 10% of the estimated maximum load was proposed in KS F 2082.

3.3. Verification of test procedure on cross-laminated timber

A CLT specimen was tested using the determined measurement area and loading protocol to verify the test

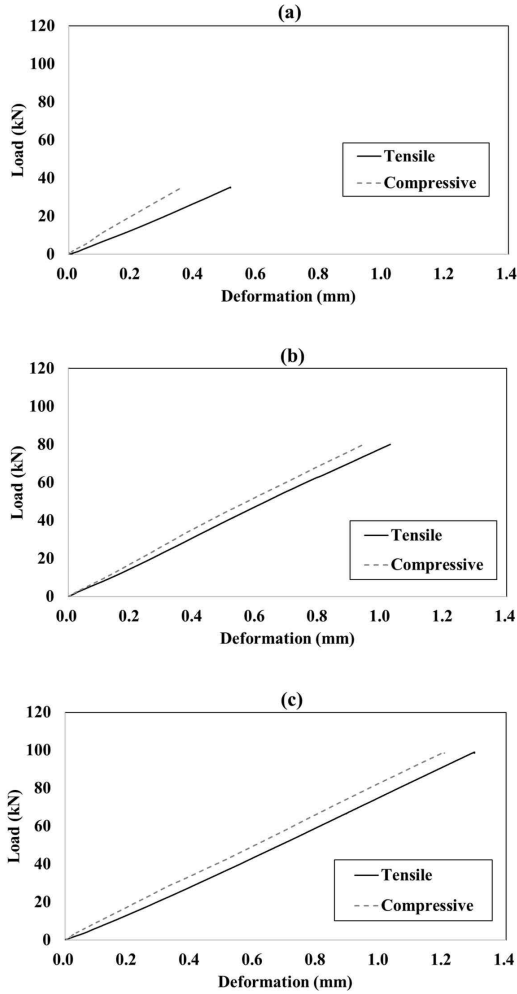


Fig. 14. Load-deformation curves of the plywood panel in (a) 1st, (b) 2nd, (c) 3rd load phase.

procedure proposed in this study. The estimated maximum load was determined based on the shear area and shear strength of the CLT panel, using the test data of Gagnon *et al.* (2014). Fig. 16 shows the load-deformation curve of the CLT panel test after preloading. Similar behaviors were observed in the tensile and compressive directions in the measurement area. The slopes of the curves in the tensile and compressive directions are listed in Table 2. The difference between the tensile and

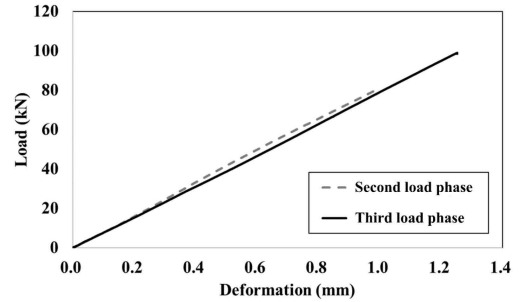


Fig. 15. Averaged load-deformation curves of the 2nd and 3rd load phase.

Table 1. Slopes of the load-deformation curves for plywood

Load phase	Tensile (kN/mm)	Compressive (kN/mm)	Difference (%) ¹⁾
1st	68.0	97.9	36.1
2nd	79.0	85.6	8.0
3rd	76.2	82.0	7.3

¹⁾ (Compressive - Tensile) / average.

compressive slopes was 2.0%, indicating that the experimental method presented in this study and KS F 2082 was applicable for generating a pure shear state and was also an effective experimental method for CLT. The in-plane shear modulus of CLT was evaluated using the formula derived in this study; the shear modulus of the CLT specimen was 693 MPa.

4. CONCLUSIONS

In this study, the process of establishing a standard test method for the in-plane shear modulus of CLT, KS F 2082, was investigated. The picture frame method was selected as the test method because it could induce a pure shear state in the test specimen. Two parts of the test procedure were examined.

First, the measurement area was determined by using

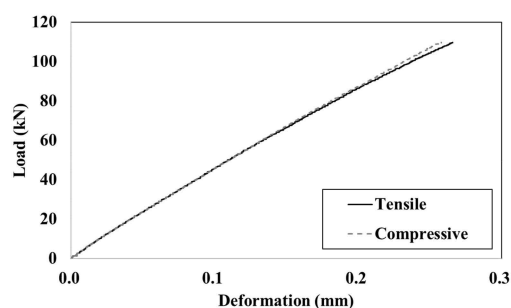


Fig. 16. Load-deformation curve of the CLT panel test. CLT: cross-laminated timber.

Table 2. The values of tensile and compressive slopes, and in-plane shear modulus of CLT

Tensile slope (kN/mm)	Compressive slope (kN/mm)	Difference (%)
404.2	396.3	2.0

CLT: cross-laminated timber.

an acrylic sheet and DIC equipment. The difference between the compressive and tensile deformations was measured at nine points representing 50%–100% of the shear area length. When the measurement area length was less than 70% of the shear area length, the difference between the tensile and compressive deformations decreased to less than 10%. Based on the results, the measurement area was specified to be within a maximum of 50% of the shear length in KS F 2082, from the viewpoint of conservatism.

Subsequently, the loading protocol was determined. Three load phases, including two preload steps, were proposed. A preload was applied to settle the test specimen into the test jig, and the test results from the acrylic sheet showed the necessity of preloading. A test on a plywood panel was conducted by applying this loading protocol, and the results demonstrated that the difference between the tensile and compressive deformations decreased as the stages progressed (36.1% in the first, 8.0% in the second, and 7.3% in the third load

phase). Considering the large difference between the tensile and compressive directions in the first load phase, a loading protocol that introduces at least one preloading stage with 10% of the estimated maximum load was proposed in KS F 2082.

A CLT specimen was tested following the determined loading protocol and measurement area. The results indicated a 2.0% difference between the tensile and compressive slopes. This shows that the experimental method proposed in this study is suitable for achieving a pure shear state and effective for testing CLT.

CONFLICT of INTEREST

No potential conflict of interest relevant to this article was reported.

ACKNOWLEDGMENT

This study was supported by the National Institute of Forest Science (Project No. 0525-20210022 and FP0000-2023-01-2024).

REFERENCES

- American Society for Testing and Materials [ASTM]. 2019. Standard Test Methods for Structural Panels in Shear Through-the-Thickness. D2719-19. ASTM International, West Conshohocken, PA, USA.
- Andreolli, M., Rigamonti, M.A., Tomasi, R. 2014. Diagonal compression test on cross-laminated timber panels. In: Quebec, QC, Canada, Proceedings of the 13th World Conference on Timber Engineering.
- Berg, S., Turesson, J., Ekevad, M., Björnfort, A. 2019. In-plane shear modulus of cross-laminated timber by diagonal compression test. *BioResources* 14(3): 5559-5572.
- Björnfort, A., Boggian, F., Nygård, A.S., Tomasi, R. 2017. Strengthening of traditional buildings with

- slim panels of cross-laminated timber (CLT). In: Istanbul, Turkey, Proceedings of the 4th International Conference on Structural Health Assessment of Timber Structures (SHATIS'17).
- Bogensperger, T., Moosbrugger, T., Schickhofer, G. 2007. New test configuration for CLT-wall-elements under shear load. In: Bled, Slovenia, Proceedings of the CIB-W18/40-21-2, pp. 1-14.
- Bosl, R. 2002. Zum nachweis des trag- und verformungsverhaltens von wandscheiben aus brettlagenholz. Ph.D. Thesis, Universität der Bundeswehr München, Germany.
- Brandner, R., Bogensperger, T., Schickhofer, G. 2013. In plane shear strength of cross laminated timber (CLT): Test configuration, quantification and influencing parameters. In: Vancouver, BC, Canada, Proceedings of the CIB-W18/46-12-2.
- Cha, M.S., Yoon, S.J., Kwon, J.H., Byeon, H.S., Park, H.M. 2022. Mechanical properties of cork composite boards reinforced with metal, glass fiber, and carbon fiber. *Journal of the Korean Wood Science and Technology* 50(6): 427-435.
- Dujic, B., Klobcar, S., Zarnic, R. 2007. Influence of openings on shear capacity of wooden walls. In: Bled, Slovenia, Proceedings of the CIB-W18/40-15-6.
- Flaig, M., Bläß, H.J. 2013. Shear strength and shear stiffness of CLT-beams loaded in plane. In: Vancouver, BC, Canada, Proceedings of the 46th CIB-W18/46-12-3.
- Gagnon, S., Mohammad, M., Munoz Toro, W., Popovski, M. 2014. Evaluation of in-plane shear strength of CLT. In: Quebec, QC, Canada, Proceedings of the 13th World Conference on Timber Engineering.
- Gubana, A. 2008. Cross laminated timber panels to strengthen wood floors. In: D'Ayala, D. and Fodde, E. (eds), Bath, UK, Proceedings of the VI International Conference on Structural Analysis of Historic Construction, pp. 949-955.
- Ha, Y.S., Lee, H.J., Lee, S.J., Shin, J.A., Song, D.B. 2023. A study on floor impact sound insulation performance of cross-laminated timber (CLT): Focused on joint types, species and thicknesses. *Journal of the Korean Wood Science and Technology* 51(5): 419-430.
- Hwang, S.W., Chung, H.W., Lee, T., Ahn, K.S., Pang, S.J., Bang, J., Kwak, H.W., Oh, J.K., Yeo, H. 2022. Monitoring of moisture and dimensional behaviors of nail-laminated timber (NLT)-concrete slab exposed to outdoor air. *Journal of the Korean Wood Science and Technology* 50(5): 301-314.
- Jöbstl, R.A., Bogensperger, T., Schickhofer, G. 2008. In-plane shear strength of cross laminated timber. In: St. Andrews, NB, Canada, Proceedings of the CIB-W18/41-12-3.
- Kang, E.C., Lee, M., Lee, S.M., Park, S.H. 2023. Mechanical properties of the oriented strand board (OSB) distributed in the Korean market. *Journal of the Korean Wood Science and Technology* 51(4): 253-269.
- Kim, K.H., Lee, H.M., Lee, M. 2024. Evaluation of adhesive characteristics of mixed cross laminated timber (CLT) using yellow popular and softwood structural lumbers. *Journal of the Korean Wood Science and Technology* 52(1): 58-69.
- Korean Standards Association. 2018. Rolled Steels for General Structure. KS D 3503. Korean Standards Association, Seoul, Korea.
- Korean Standards Association. 2021. Structural Plywood. KS F 3113. Korean Standards Association, Seoul, Korea.
- Korean Standards Association. 2023. Measurement of In-plane Shear Modulus for Cross Laminated Timber. KS F 2082. Korean Standards Association, Seoul, Korea.
- Kreuzinger, H., Sieder, M. 2013. Einfaches prüfverfahren zur bewertung der schubfestigkeit von kreuzlagenholz/brettsperrholz. *Bautechnik* 90(5): 314-316.

- Lee, H.W., Jang, S.S. 2023. Lateral resistance of reinforced light-frame wood shear walls. *Journal of the Korean Wood Science and Technology* 51(1): 58-66.
- Lee, I., Oh, W. 2023. Flexural modulus of larch boards laminated by adhesives with reinforcing material. *Journal of the Korean Wood Science and Technology* 51(1): 14-22.
- Lukacs, I., Björnfort, A., Tomasi, R. 2019. Strength and stiffness of cross-laminated timber (CLT) shear walls: State-of-the-art of analytical approaches. *Engineering Structures* 178: 136-147.
- Ministry of Land, Infrastructure and Transport. 2022. Design of Connections in Timber Construction. KDS 41 50 30. Ministry of Land, Infrastructure and Transport, Sejong, Korea.
- Oh, J.W., Park, K.S., Kim, H.S., Kim, I., Pang, S.J., Ahn, K.S., Oh, J.K. 2023. Comparative CO₂ emissions of concrete and timber slabs with equivalent structural performance. *Energy and Buildings* 281: 112768.
- Oh, S. 2022. Experimental study of bending and bearing strength of parallel strand lumber (PSL) from Japanese larch veneer strand. *Journal of the Korean Wood Science and Technology* 50(4): 237-245.
- Ozdemir, M.F., Maras, M.M., Yurtseven, H.B. 2023. Flexural behavior of laminated wood beams strengthened with novel hybrid composite systems: An experimental study. *Journal of the Korean Wood Science and Technology* 51(6): 526-541.
- Riberholt, H. 1984. Simplified static analysis and dimensioning of trussed rafters, part 1. In: Rapperswil, Switzerland, Proceedings of the CIB-W18/17-14-2.
- Song, D., Kim, K. 2022. Influence of manufacturing environment on delamination of mixed cross laminated timber using polyurethane adhesive. *Journal of the Korean Wood Science and Technology* 50(3): 167-178.
- Song, D.B., Kim, K.H. 2023. Influence of composition of layer layout on bending and compression strength performance of larix cross-laminated timber (CLT). *Journal of the Korean Wood Science and Technology* 51(4): 239-252.
- Trisatya, D.R., Santoso, A., Abdurrachman, A., Prastiwi, D.A. 2023. Performance of six-layered cross laminated timber of fast-growing species glued with tannin resorcinol formaldehyde. *Journal of the Korean Wood Science and Technology* 51(2): 81-97.
- Turesson, J., Berg, S., Ekevad, M. 2019a. Impact of board width on in-plane shear stiffness of cross-laminated timber. *Engineering Structures* 196: 109249.
- Turesson, J., Björnfort, A., Berg, S., Ekevad, M., Tomasi, R. 2019b. Picture frame and diagonal compression testing of cross-laminated timber. *Materials and Structures* 52(4): 66.
- Wallner, G. 2004. Versuchstechnische ermittlung der verschiebungskenngrößen von orthogonal verklebten brettlamellen. Diploma Thesis, Graz University of Technology, Austria.